The IRIDIUM Main Mission Antenna Concept

J. J. Schuss, J. Upton, B. Myers, T. Sikina, A. Rohwer, P. Makridakas,
R. Francois, L. Wardle, and R. Smith

(Invited Paper)

***Abstract*—The design of a novel phase array panel that provides the *L*-band satellite to ground links for the IRIDIUM global communications system is presented. Key components and aspects of this phase array antenna are discussed including the beamforming architecture, radiated intermodulation products, the patch radiators, and the T/R module. The strategy for minimizing dc power consumption over a large range of multicarrier RF output power is described. Finally, test results showing compliant array operation are summarized.**

***Index Terms*—Antenna arrays, phased arrays.**

I. Array Overview

MOTOROLA has proposed and deployed the IRIDIUM[1] system, whose objective is to achieve a global personal satellite communications system based on a constellation of 66 satellites placed in low earth orbit. These satellites are positioned in six polar orbital planes with 11 satellites plus one spare per plane. A key component of each of these satellites (shown in Fig. 1) is the main mission antenna (MMA), which consists of three fully active phased-array panels and provides the *L*-band link from the satellite to the ground user. Each phased-array panel produces 16 fixed simultaneous beams for a total of 48 beams per satellite with users on the ground communicating with the IRIDIUM network through the satellite whose beam covers the user. As satellites in the network travel along their orbits, the ground user is handed off from beam to beam and from satellite to satellite, depending on which particular beam provides the best link margin to the user. All satellites in the system are linked into a network that makes this handoff transparent to the user. The IRIDIUM link quality and capacity requirements, including the requirement of communicating with hand-held phones having low-gain antennas, place stringent specifications on the MMA. The MMA must be capable of simultaneously radiating multiple carriers into multiple beams with high efficiency and linearity as well as being lightweight and able to function in the thermal and radiation environment of space. Furthermore, beam coverage must be optimized to yield the highest possible link margin consistent with the size of the antenna panels and the budgeted RF power per carrier. In particular, the requirements on maximum dc power draw by the MMA, both peak and orbit averaged, are particularly severe and require efficient operation and low dc bias power over a 20-db range in radiated RF power.

These requirements have led to the synthesis of a novel electromagnetic and structural architecture for the MMA panels. The features of the MMA panel include:

- multiple simultaneous-shaped beam operation on transmit and receive with optimized beam coverage for maximum link margin;
- lightweight high-efficiency patch radiators and beamformer;
- lightweight high-efficiency linear pseudomorphic high-electron mobility transistor (PHEMT)-based T/R modules;
- low-noise redundant dc power/data distribution system;
- a lightweight structure designed for the thermal and radiation environment of space and the mechanical launch environments.

These features have been combined together into an integrated phased-array design that meets the stringent IRIDIUM performance and cost requirements.

The architecture of the MMA panel is shown in Figs. 2 and 3. Each array consists of over 100 lightweight patch radiators, each of which is driven by a T/R module, which are in turn collectively excited by an optimized beamformer network. The beamformer network serves to form the 16 optimized shaped beams for both transmit and receive operation with the T/R modules serving to maintain high G/T in receive operation and efficient EIRP generation for transmit operation. The satellite can receive or transmit through each beamport, with each beamport connection providing for the RF access to a particular fixed beam. In general, several or all beams can be utilized at once in either transmit or receive operation with the only limitation being the MMA capacity constraints on transmit. A T/R module is provided at each beamport input to maintain system noise figure on receive and to provide for the required RF drive power on transmit. One additional T/R module is placed in the array as part of the RF BITE function; RF BITE, which diagnoses the status of the MMA RF chain, is obtained by transmitting from a single element and measuring the response on an adjacent element through its mutual coupling coefficient. The RF BITE T/R module provides the correct level of RF excitation for this procedure and facilitates the determination of the loop gain by use of its precision attenuator.

Manuscript received April 29, 1998; revised April 9, 1999.

J. J. Schuss, J. Upton, B. Myers, T. Sikina, A. Rohwer, P. Makridakas, R. Francois, and L. Wardle are with the Raytheon Company, Sudbury, MA 01776 USA.

R. Smith is with Motorola, Inc., Chandler, AZ 85248 USA.

Publisher Item Identifier S 0018-926X(99)05435-6.

[1] IRIDIUM is a registered trademark and service mark of Iridium LLC.

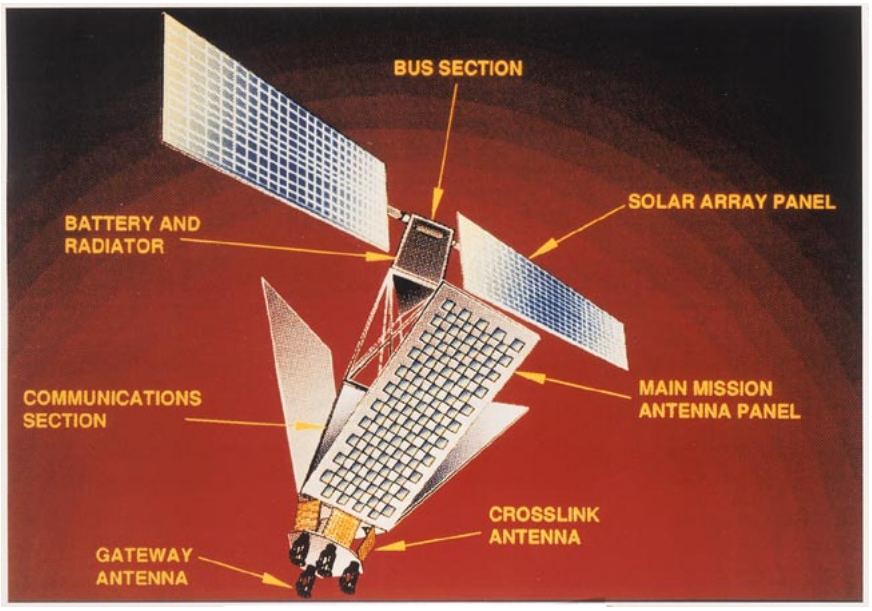

Fig. 1. IRIDIUM space vehicle.

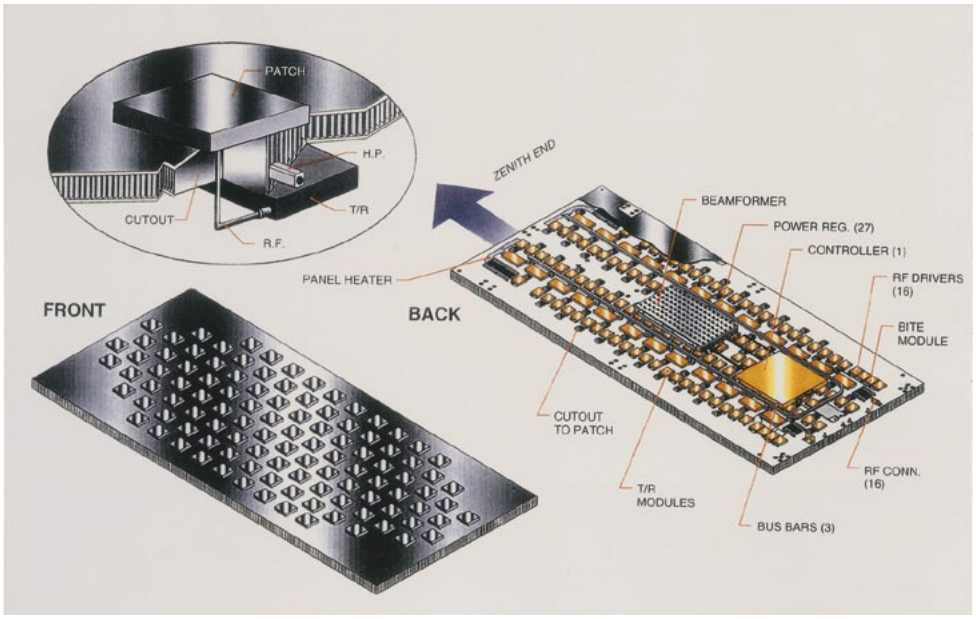

Fig. 2. MMA panel construction.

DC power to array components is provided by a bank of efficient hybrid construction power regulators. These power regulators, which are redundant, condition the 28-V power-bus input from the satellite and provide for the array bias voltages. In particular, the bias for the drains of the power FET's in the array T/R modules is provided for by a subgroup of power regulators. This bias voltage, which draws the major part of the array's dc power in transmit operation, can be changed in order to reduce power draw during periods of low traffic. A dual redundant array controller is also built into the panel, which coordinates array operation as commanded by the satellite. Upon one of the dual sections of the controller being enabled, the array will be booted up, the health and status of all components verified, and the array put into telephone mode. Finally, a heater is placed on the MMA and powered by the 28-V satellite power bus. This heater can be enabled to maintain minimum MMA temperatures during low traffic or on orbit storage modes.

The array mechanical structure is based on a 74 in $\times$ 34 in aluminum honeycomb panel that has been sized for the launch environments. The power regulators and the T/R modules are bonded onto this structure so as to obtain a good thermal and mechanical attachment. The panel contains two heat pipes that are routed so as to be bonded to the bottom plate of each T/R module, as shown in Fig. 2. The power FET's of each module are placed above these heat pipes, which serve to efficiently route waste heat out of the power amplifiers and into the array structure.Once this heat is distributed onto the

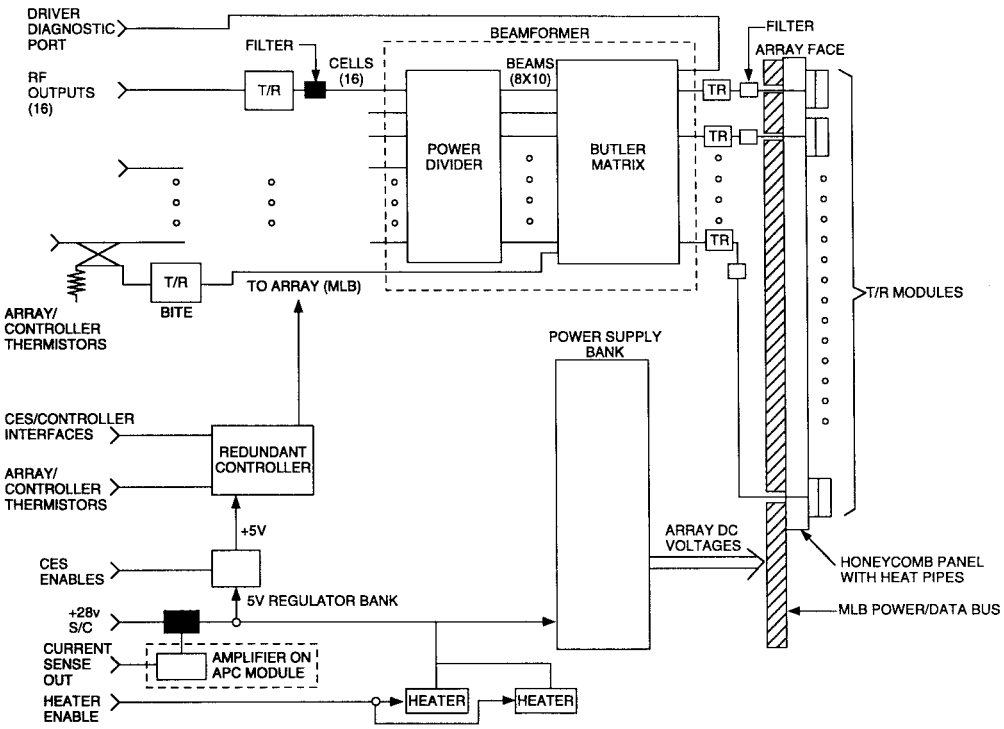

Fig. 3. MMA panel architecture.

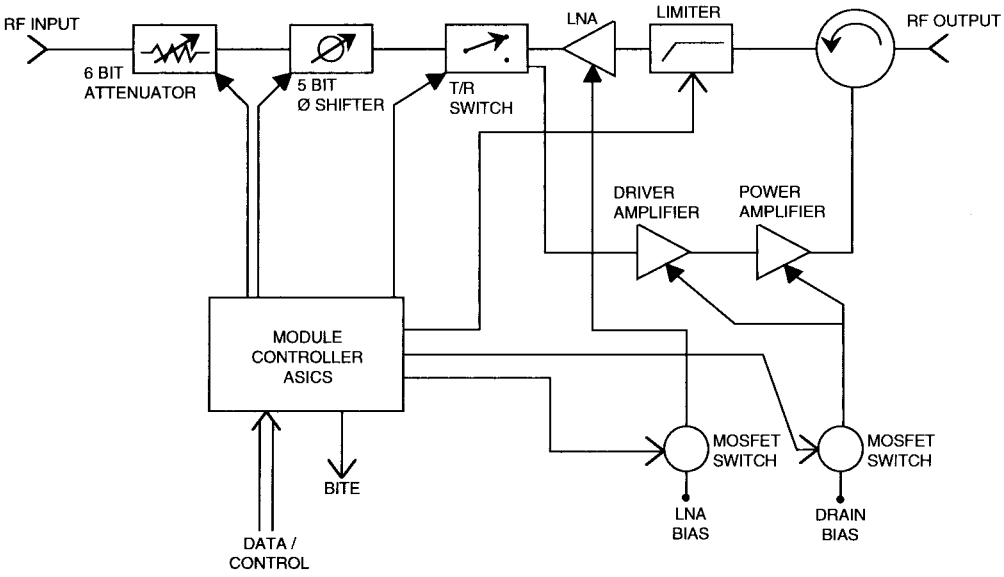

Fig. 4. Schematic of T/R module.

array, it is radiated out the front surface of the panel, which is coated with flexible optical solar reflector (FOSR). The FOSR provides for rejection of solar loading simultaneously with high thermal emissivity. The panel has been thermally designed to operate through periods of high traffic using this method of heat distribution and rejection and to limit peak T/R module temperatures to levels within the T/R module's specification temperature range.

Fig. 4 is a schematic of the array T/R modules. Each module has both an low-noise amplifier (LNA) for receive operation and a power amplifier chain for transmit operation. The module can be operated in either transmit, receive, or standby mode as selected by the array controller and coordinated by the module controller chip in each T/R module. A 5-bit phase shifter and a 6-bit attenuator are provided for in each T/R module; these are used for array calibration and temperature compensation for each mode of operation. The power amplifiers in the T/R module are based on PHEMT FET's and have an extremely efficient design that permits for low bias powers when the module is operated at low output powers.

Figs. 5 and 6 show, respectively, the front (radiator) surfaces and the rear (component) surfaces of an MMA panel. Other key features of the array will be discussed in more detail below.

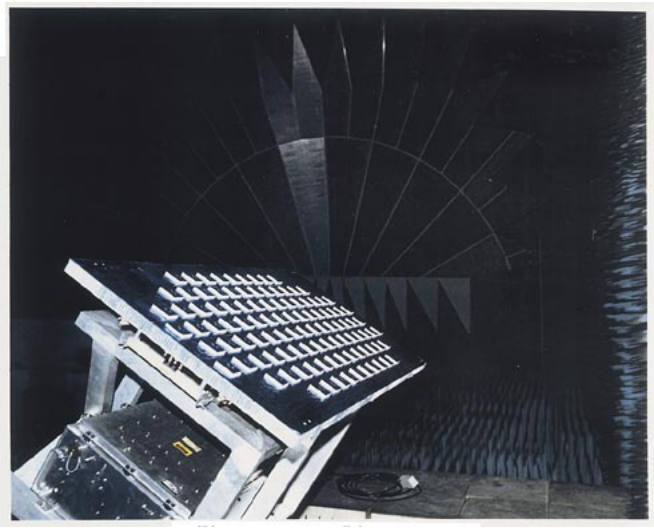

Fig. 5. Radiator face of MMA panel (in compact antenna range).

II. Beamforming Architecture

The array beamforming strategy is based upon an RF feed composed of crossed Butler matrices [1] with the different beamlets of the Butler matrices combined into the desired 16 final beams. This concept is schematically presented in Fig. 7, which shows the IRIDIUM beamformer [2] being composed of eight 16 × 16 Butler matrices fed in turn by ten 8 × 8 orthogonal Butler matrices. The resulting beamlets of this feed fill the scan volume of the array, as shown in Fig. 7. Here is the cosine of the angle between the scan direction and the x axis (along the short direction of the array) and v is the cosine of the angle between the scan direction and the y axis (along the long direction of the array). The power divider then combines different beamlets as required to form the required 16 far-field beam patterns. The requirement on the 16 beams of the array is to meet a stringent effective isotropic radiated power (EIRP) specification over the coverage area on the earth. This was accomplished using an iterative method of projections synthesis routine [3]. The main beam and sidelobes of each beam were constrained to be within desired far-field masks. Furthermore, the aperture amplitude distribution was constrained to be within a max/min range. This latter constraint was important, as the beams near nadir subtend large solid angles and would cause high peak to average power densities on the array face if this issue was not addressed. The aperture illumination function at the element level was then iterated to arrive at the best fit to the far-field pattern requirements, consistent with the max/min power density requirements on the array face. Finally, the best far-field pattern was sampled at the beamlet peaks to obtain the complex weighting amplitudes for each beamlet in a beam. Fig. 8 shows the results of this synthesis for the 16 beams realized for the MMA panel as measured on the first qualification panel. Note that in Fig. 8, X Ground and Z Ground are earth based axes and Fig. 8 shows the mapping of the 16 beams of the MMA panel onto the surface of the earth. $X-\text{Ground}=0$ and $Z-\text{Ground}=0$ corresponds to the earth location directly beneath the satellite. These beams meet the IRIDIUM EIRP and G/T requirements with margin.

III. Nonlinear Effects

A key issue in the design of the MMA is maintaining far-field intermodulation products at least 18 db below the desired far-field carriers. While this intermdoulation distortion product can be measured and characterized easily for a component on the bench, it can only be measured in the far field with an array fully populated with its T/R modules and driven to the required EIRP level. Since this latter measurement is accomplished late in the design cycle, there is a need to predict the array's intermodulation products during the design phase and to tailor the T/R module requirements so as to meet specifications. These predictions were carried out early in the MMA design to assure margin in the final array against intermodulation product requirements.

In general, the input to a T/R module in the MMA is a noise-like signal that is composed of many carriers, randomly phased with respect to each other

$$V_{\text{in}}(\omega)=\sum_{i=1}^{N}V_i e^{j\phi_i}\delta(\omega-\omega_i) \tag{1}$$

where V_i is the amplitude of carrier i, ϕ_i is its phase, and ω_i is its angular frequency. This spectral domain signal can be rewritten in the time domain

$$V_{\text{in}}(t)=\sum_{i=1}^{N}V_i e^{j(\omega_i t+\phi_i)}. \tag{2}$$

The T/R module can be characterized by a gain G(V) and a phase Φ(V), which describes the T/R module's nonlinear response to the slowly varying envelope of the noise-like RF signal. This results in an output voltage

$$V_{\text{out}}(t)=G(|V_{\text{in}}(t)|)e^{j\Phi(|V_{\text{in}}(t)|)}V_{\text{in}}(t) \tag{3}$$

which can be Fourier transformed back to the frequency domain

$$V_{\text{out}}(\omega_k)=\sum_{i=1}^{N_t}V_{\text{out}}(t_i)e^{-j\omega_k t_i} \tag{4}$$

where N_t is the number of time samples used. This latter $V_{\text{out}}(\omega_k)$ is the spectral component of the output of the T/R module at angular frequency ω_k. These spectral components of the array T/R modules can then be combined in the array far field to arrive at the spectral and angular patterns of the array. This spectral output of the array can be decomposed into a linear desired output and a nonlinear distortion output as follows:

$$V_{\text{out}}^{\text{Non}}(\omega_k)=1/2[V_{\text{out}}(\omega_k,+V_k),+V_{\text{out}}(\omega_k,-V_k)] \tag{5a}$$

$$V_{\text{out}}^{\text{Lin}}(\omega_k)=1/2[V_{\text{out}}(\omega_k,+V_k),-V_{\text{out}}(\omega_k,-V_k)] \tag{5b}$$

where $V_{\text{out}}^{\text{Lin}}(\omega_k)$ is the desired linear output and $V_{\text{out}}^{\text{Non}}(\omega_k)$ is the nonlinear distortion output. Here it should be noted that $V_{\text{out}}(\omega_k,+V_k)$ corresponds to the spectral outputs of a

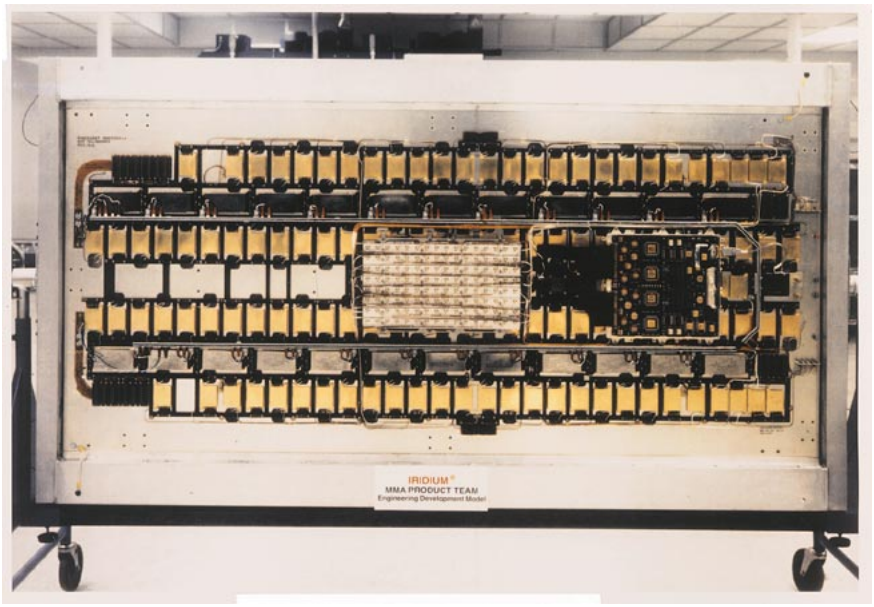

Fig. 6. Component face of MMA panel (with thermal blanket removed).

positive V_k input excitation and $V_{\text{out}}(\omega_k, -V_k)$ corresponds to the spectral output with all V_k's having their signs reversed. This calculation must be repeated for at least 10 to 20 seeds of the random phases of the array input carrier voltages and the results averaged in power to arrive at the array linear and nonlinear patterns as a function of frequency.

Such calculations have been extensively carried out and have predicted compliance with IRIDIUM requirements. In general, far-field measurements of the MMA panels have always shown intermodulation products at least 20 db below the linear products.

IV. Patch Radiator

Fig. 9(a) and (b) shows the patch radiator developed for the MMA, which is manufactured as a separate component and bonded onto the MMA panel during array assembly. This radiator is built as one assembly and contains internal to the radiator the matching and polarizing networks needed for the MMA application; a single 50-Ω input connector is provided on the underside of the patch for connection to the T/R module. The radiator was designed to be fabricated in one bonding step and in general was optimized for mass production. The radiator cavity is loaded with an artificial dielectric substrate whose weight is approximately one tenth that of teflon, but which has a dielectric constant of approximately two. This dielectric constraint is needed to obtain the desired scan and polarization performance of the array.

Key requirements that the patch radiator had to meet were to maintain low weight and to permit efficient heat radiation out the front face of the array during peak traffic loads. Weight was greatly reduced by the use of the artificial dielectric, which provided for high-scan performance while weighting much less than teflon. Weight was further reduced by cutting away the entire dielectric structure everywhere except under the patch itself; this can be done because the dielectric is only needed under the patch to set the patch radiator dimensions and has

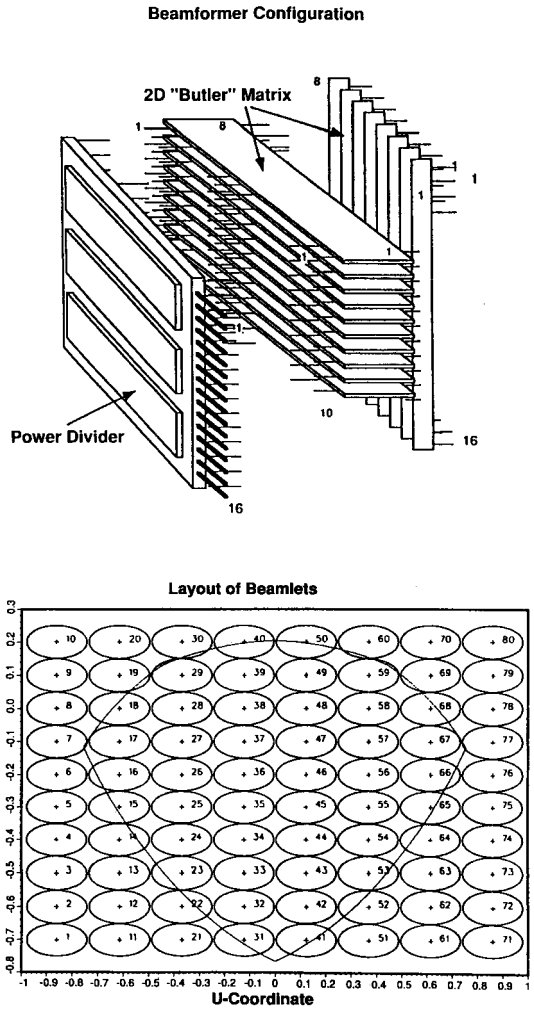

Fig. 7. Beamformer architecture.

no efficacy on the remainder of the array face. This feature was also critical in providing for heat radiation out the front face of the array. Because the dielectric is cut away, most of

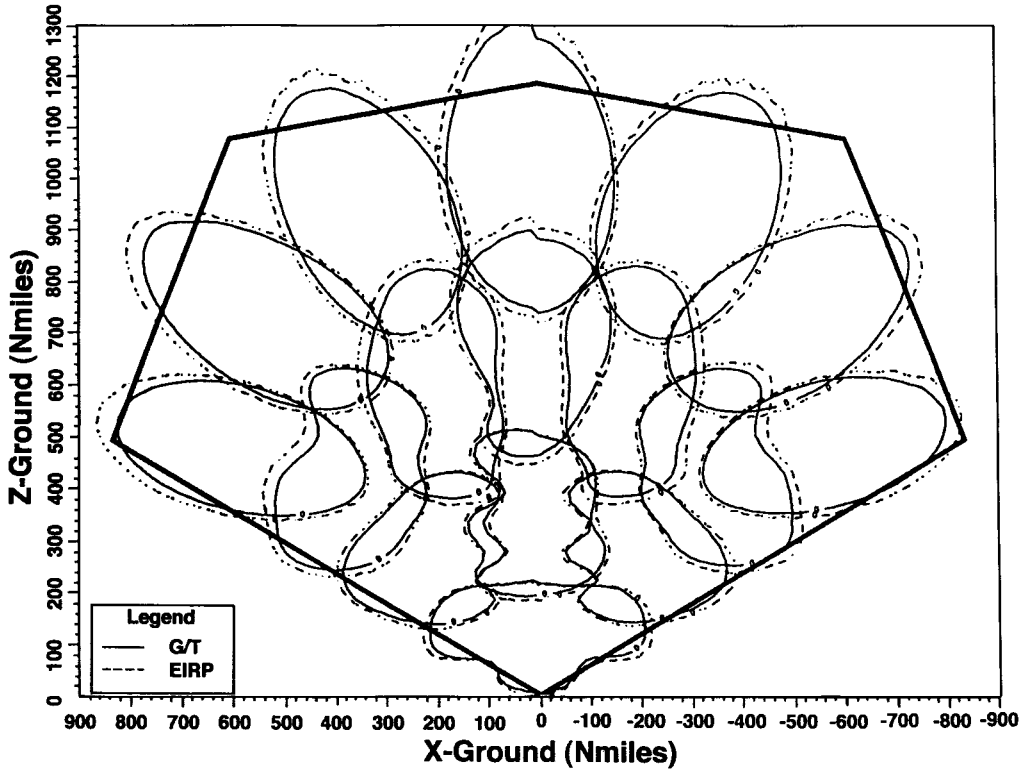

Fig. 8. Transmit and receive beams for qualification panel.

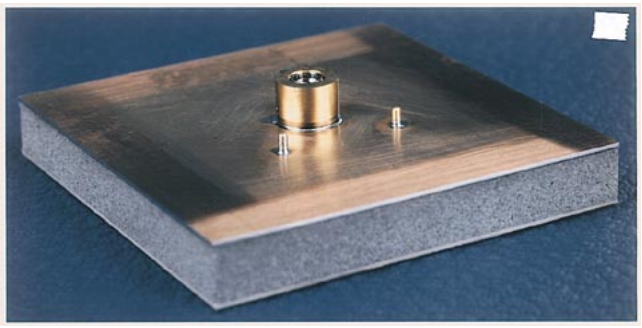

(a)

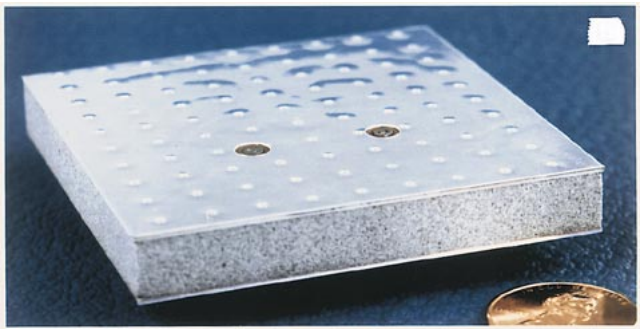

(b)

Fig. 9. (a) and (b) Patch radiator.

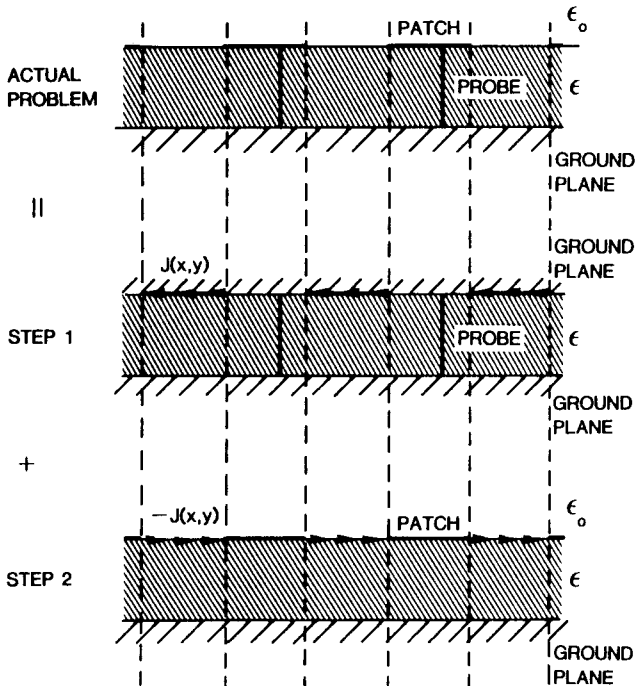

Fig. 10. Two-step method.

the array ground plane is bare and can be covered by FOSR. The FOSR does not impact RF operation, but allows a direct path for heat loss into space without having to penetrate an insulating dielectric layer. The resulting design is much lighter than a conventional patch array and easily maintains peak MMA temperatures below required limits during peak loads at end of life conditions.

The numerical design and optimization of MMA patch radiator was accomplished using a numerical computer code developed by Raytheon that rigorously models patch radiator performance in the infinite array environment. This code combines two earlier treatments of patch radiator arrays to

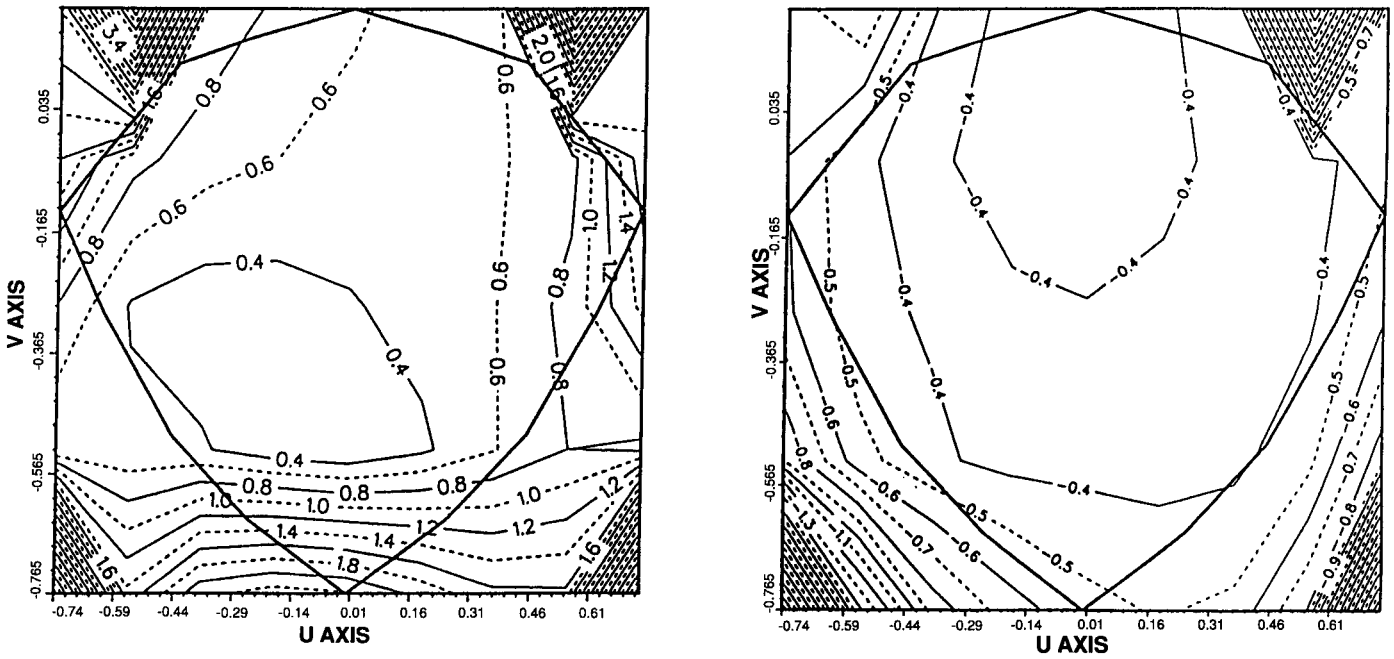

(a) (b)

Fig. 11. (a) Predicted radiator axial ratio. (b) Total loss versus scan angle.

arrive at an efficient and accurate electromagnetic model. The code uses a method of moments technique for determining the patch radiator currents and the probe impedances for probe-fed patch radiators [4]–[7]. However, it also employs a two-step technique for handling the probe excitation currents [8]–[10]. These probe currents and their associated currents on the patch surfaces are nearly singular in comparison with the resonant mode-patch currents; these near singular currents would require a large number of basis functions to be properly represented, which would then greatly slow execution of the numerical code if handled without the use of a two-step technique. In the two-step technique, the nearly singular probe currents are handled analytically and a well-behaved equivalent current source is derived for use in a method of moments code. Fig. 10 illustrates this process. In step one, the problem of an infinite array of proves between two ground planes is solved analytically. The negative of the currents on the upper ground plane in the region that corresponds to the gaps between patches is obtained and used as a source excitation for the system of step 2, which consists of an infinite array of probeless patches. The step 2 problem does not contain any singular currents and converges rapidly in a method of moments code. It can be readily seen that the linear combination of steps 1 and 2 corresponds to the original problem. The result of this method is an accurate rapidly converging numerical model that facilitates the optimization of patch radiator parameters against array requirements [11]. This method can handle both rectangular and triangular lattice arrays; the triangular lattice array is addressed as a combination of two interleaved rectangular arrays whose solutions are linearly added.

It should be noted that this model includes surface wave effects and radiator asymmetries and explicitly takes into account the patch radiator matching network in predicting element performance. This latter effect is critical in predicting radiator performance. In the case of a dual probe-fed circularly polarized patch radiator, the two probes are, in general, not identical in their effective impedances. If this effect is not taken into account, incorrect predictions of axial ratio will be obtained. A complete cascade of the patch radiator scattering matrix, together with the matching circuit, must be executed if patch performance is to be properly modeled [11].

Fig. 11(a) and (b) shows the axial ratios and total loss (excluding the polarizer ohmic loss) for the MMA patch radiator over its scan volume in sine space, predicted using this numerical method. These calculations predict radiator losses less than 0.5 db and axial ratios below 1.0 db over almost the entire coverage area of a panel. Note that the solid line outlines the scan volume and the units of the contour plot are in decibels. Fig. 12 shows a measured azimuthal embedded element pattern for this radiator, which is consistent with the predictions. An extensive series of embedded element gain, pattern, and mutual coupling measurements were carried out, which have confirmed the radiator design predictions.

In order to validate both the beamformer design and the radiator design, a passive-array pattern test was carried out early in the MMA design phase to check the fidelity of the measured array patterns. This test was carried out by connecting a beamformer directly to the patch radiators of an MMA panel without intervening T/R modules. Fig. 13 shows a comparison of the measured and predicted far-field patterns of this passive array. Both the beam shapes (shown), directivities, antenna gains at beam peaks, and sidelobe levels were in excellent agreement with predictions. This test served to validate the electromagnetic design of the MMA prior to starting integration with the active components.

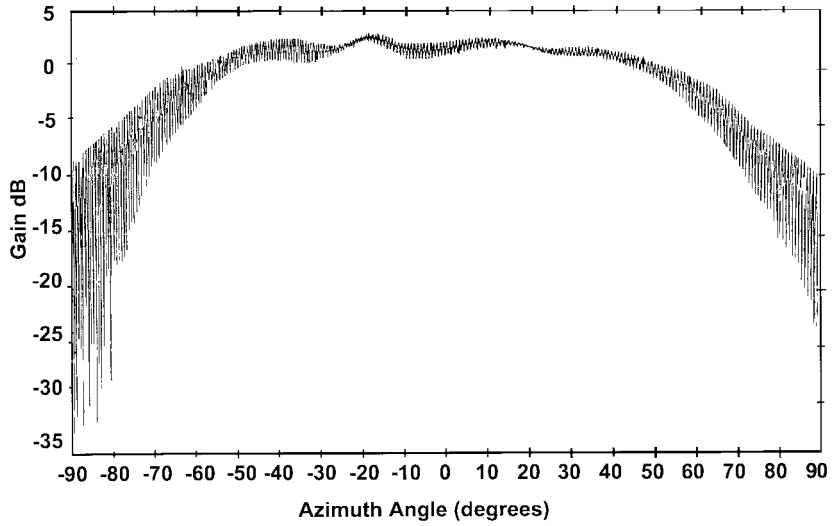

Fig. 12. Measured embedded element pattern (azimuth, 1.621 GHz).

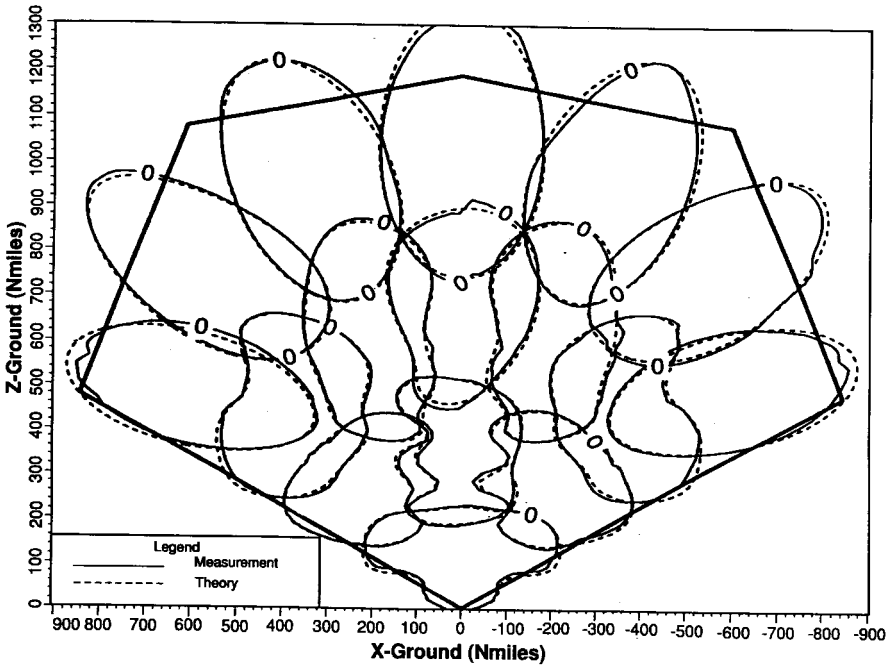

Fig. 13. Comparison of predicted and measured far-field pattern of passive test array.

V. DC Power Consumption

One of the most difficult requirements to meet for the MMA has been the dc power consumption specification, especially at low RF output powers. This latter dc bias power at low traffic dominates the total consumed dc power when averaged over several orbits as most of the time it is anticipated that the satellite will not be operating at peak capability. A conventional GaAs power amplifier (PA)-based array similar to the MMA panel would consume approximately ten times as much power as permitted to the MMA when turned on but not transmitting RF. Thus, an order of magnitude decrease in bias power is required over that of a conventional array. The MMA has achieved this significant decrease in dc power consumption by taking the following steps:

- use of pseudomorphic high electron mobility (PHEMT)-based power amplifiers (1.67-factor improvement);
- use of an improved efficiency PA architecture (2.0-factor improvement);
- rebiasing PA's during low traffic periods (2.0-factor improvement);
- use of five different module sizes tailored to the peak RF output power at the T/R modules' location (2.0-factor improvement).

In total, these factors indicate a total improvement over a conventional array of approximately 13. This improvement factor allows the MMA to meet the IRIDIUM dc power consumption goals. Further power reductions are expected in the future as a result of continuous improvement activities.

VI. Array Validation

Early in the program one engineering model panel and five qualification model panels were built and tested. Two of the qualification panels were subjected to extensive environmental qualification tests and design verification tests. In general, the arrays were shown to meet or exceed all IRIDIUM requirements. Pattern testing has indicated that the arrays meet the IRIDIUM G/T, EIRP, and sidelobe specifications. Furthermore, intermodulation products have been shown to be more than 20 db below the carrier outputs. Full-scale production of these MMA's is now in process and satellites containing MMA's have been placed into orbit. Over 300 panels will have been delivered in support of the constellation needs of the IRIDIUM system.

References

[1] J. Butler and R. Lowe, "Beamforming matrix simplifies design of electronically scanned antennas," *Electron. Design*, vol. 9, pp. 170–173, 1961.

[2] Beamformer designed, fabricated, Anaren Microwave, Syracuse, NY.

[3] O. M. Bucci, G. Franceschetti, G. Mazzarella, and G. Panariello, "Intersection approach to array pattern synthesis," *Proc. Inst. Elect. Eng.*, vol. 37, pt. H, pp. 349–357, Dec. 1990.

[4] D. M. Pozar, "Input impedance and mutual coupling of rectangular microstrip antennas," *IEEE Trans. Antennas Propagat.*, vol. AP-30, p. 1191, Nov. 1982.

[5] ———, "Considerations for millimeter wave printed antennas," *IEEE Trans. Antennas Propagat.*, vol. AP-31, p. 740, Sept. 1983.

[6] D. M. Pozar and D. H. Schaubert, "Scan blindness in infinite phased arrays of printed dipoles," *IEEE Trans. Antennas Propagat.*, vol. AP-32, p. 602, June 1984.

[7] ———, "Analysis of an infinite array of rectangular microstrip patches with idealized probe feeds," *IEEE Trans. Antennas Propagat.*, vol. AP-32, p. 1101, Oct. 1984.

[8] C. C. Liu, J. Shmoys, and A. Hessel, "*E*-plane performance tradeoffs in two-dimensional microstrip-patch element phased arrays," *IEEE Trans. Antennas Propagat.*, vol. AP-30, p. 1201, Nov. 1982.

[9] C. C. Liu, J. Shmoys, A. Hessel, J. D. Hanfling, and J. M. Usoff, "Plane wave reflection from microstrip patch arrays—Theory and experiment," *IEEE Trans. Antennas Propagat.*, vol. AP-33, p. 426, Apr. 1985.

[10] C. C. Liu, Jerry Shmoys, and A. Hessel, "Performance of probe-fed microstrip-patch element arrays," in *Proc. Phased Arrays Symp.*, Bedford, MA, Oct. 1985, p. 157.

[11] J. J. Schuss, "Numerical design of patch radiator arrays," *Electromagn.*, vol. 11, pp, 47–68, 1991.

Jack J. Schuss was born in Jersey City, NJ, in 1952. He received the B.S. degree in electrical engineering from the Massachusetts Institute of Technology (MIT), Cambridge, in 1973, and the Ph.D. degree in astrophysical sciences from Princeton University, NJ, in 1977.

From 1977 to 1983, he worked at the MIT Plasma Fusion Center studying RF heating and current drive in tokamak plasmas. Since 1983 he has worked at Raytheon Company on numerous antenna, phased-array, and solid-state development efforts, and has the rank of Consulting Engineer. He led the engineering team that developed and transitioned to production the IRIDIUM main mission antennas, which are now deployed in orbit. He is currently Director of Engineering at Raytheon Microelectronics, where he is involved in the development of solid-state components and subsystems for phased-array antennas and other wireless systems.

Dr. Schuss was named recipient of the American Physical Society 1984 Award for Excellence in Plasma Physics Research.

J. Upton, photograph and biography not available at the time of publication.

B. Myers, photograph and biography not available at the time of publication.

T. Sikina, photograph and biography not available at the time of publication.

A. Rohwer, photograph and biography not available at the time of publication.

P. Makridakas, photograph and biography not available at the time of publication.

R. Francois, photograph and biography not available at the time of publication.

L. Wardle, photograph and biography not available at the time of publication.

R. Smith, photograph and biography not available at the time of publication.